Growth of crystalline γ-Al_2O_3 on Si by molecular beam epitaxy: Influence of the substrate orientation

C. Merckling[a)]
STMicroelectronics, 850 Rue Jean Monnet, 38926 Crolles Cedex, France and INL, UMR5270/CNRS, Ecole Centrale de Lyon, 36 Avenue Guy de Collongue, 69134 Ecully, France

M. El-Kazzi, G. Saint-Girons, and G. Hollinger
INL, UMR5270/CNRS, Ecole Centrale de Lyon, 36 Avenue Guy de Collongue, 69134 Ecully, France

L. Largeau and G. Patriarche
LPN, UPR20/CNRS, Route de Nozay, 91460 Marcoussis, France

V. Favre-Nicolin
CEA/DRFMC/S2M, 17 Rue des Martyrs, 38054 Grenoble, France and Université Joseph Fourier Grenoble 1, BP 53, 38041 Grenoble Cedex 9, France

O. Marty
INL, UMR5270/CNRS, Université Claude Bernard, 8 Rue André-Marie Ampère, Campus de la Doua, 69622 Villeurbanne, France

(Received 12 March 2007; accepted 1 June 2007; published online 16 July 2007)

This work reports on the molecular beam epitaxy of high quality single crystal γ-Al_2O_3 thin films on Si(001) and Si(111) substrates. For both substrate orientations, film surfaces are found to be smooth and the oxide-Si interfaces are atomically abrupt without interfacial layers. Reflection high energy electron diffraction, x-ray diffraction, and transmission electronic microscopy characterizations were used to study the epitaxial relationship and the structural quality of the γ-Al_2O_3 layers depending on the Si substrate orientation. On Si(111), the alumina layers present a high crystalline quality. Evidence is made for a "two-for-three" unit cell indirect epitaxial relationship between γ-Al_2O_3 and Si(111). On Si(001), after a transition from cubic to hexagonal surface symmetry, the growth planes of γ-Al_2O_3 change from (001) to (111) leading to a bidomain growth. © *2007 American Institute of Physics*. [DOI: 10.1063/1.2753684]

I. INTRODUCTION

The rapid progress of the performances of complementary metal-oxide-semiconductor (CMOS) systems relies today on the downscaling approach, which mainly consists in reducing the size of the devices to increase the speed and density of the systems. However, this strategy is limited due to the apparition of intrinsic parasitic effects related to the very small thicknesses and sizes involved in the devices. Among these limiting effects, tunneling of charge carriers through nanometer thick gate oxides has been shown to strongly affect the performances of metal-oxide-semiconductor field effect transistors. Therefore, solutions have to be found to overcome this limitation. In this context, high-*k* oxides attract much attention due to their potentiality in replacing SiO_2 as a gate oxide in the future generations of CMOS devices. Several groups have focused their researches on the epitaxial growth of such oxides on Si. As compared to amorphous layers, crystalline oxides could therefore allow a better control of the Si/oxide interface and an atomic scale control of the oxide thickness. From a more general point of view, the monolithic epitaxial growth of complex oxide/semiconductor heterostructures could also open the way to the large scale integration of high performance micro-optoelectronic functionalities on Si wafers. The epitaxial growth of several rare-earth binary oxides and of perovskites (like $SrTiO_3$) has already been demonstrated.[1–5] However, these oxides are not stable enough with respect to Si and are not compatible with the thermal budget of the CMOS process: interfacial reactions occur in the 500–1000 °C temperature range that lead to the formation of SiO_2, silicates, or silicides. These interfacial layers degrade the electronic performances of the oxide/Si stack. Al_2O_3 has a moderate dielectric constant (~11) but is thermodynamically stable against silicon and SiO_2 and consequently should lead to abrupt interfaces on Si. This oxide is therefore a good candidate to be used directly as a gate oxide or as a thin buffer barrier when combined with amorphous or epitaxial oxides of higher dielectric constant.[6,7] Several groups have already reported on the epitaxial growth of cubic γ-Al_2O_3 films on Si(111) and with more difficulties on Si(001) except when chemical vapor deposition is used.[8–14] In a recent work, we have presented a study of the growth mechanism of γ-Al_2O_3 on (001)-oriented Si substrate.[14] In the present study, we show that high quality epitaxial γ-Al_2O_3 films can be prepared either on Si(001) and Si(111) by molecular beam epitaxy (MBE) growth. A detailed structural analysis of Al_2O_3 layers grown on Si(111) has been carried out, similar as the one presented in Refs. 9 and 12. Al_2O_3 layers grown on Si(001) have also been studied on the basis of reflection high energy electron diffraction (RHEED), grazing incidence x-ray Diffraction (GIXRD), and transmission electron mi-

[a)]Electronic mail: clement.merckling@ec-lyon.fr

croscopy (TEM) experiments that allow deducing in-plane epitaxial relationships between γ-Al_2O_3 and Si, and exhibit a single domain growth on Si(111) compared with the bidomain growth on Si(001) of the alumina layer.

II. EXPERIMENT

The epitaxial Al_2O_3 layers were grown in a Riber 2300 MBE reactor equipped with a 30 kV RHEED system and a camera, which allows specular beam intensity and real-time streak separation recording. The Al_2O_3 films were prepared by electron gun evaporation of single crystal Al_2O_3 under molecular oxygen. The Al_2O_3 growth rate was controlled *in situ* using a mass spectrometer and is usually around 7 Å min^{-1}. The Si substrates were first cleaned in a HF:H_2O (1:10) solution, then chemically oxidized in a H_2SO_4:H_2O_2 (2:1) solution, and finally etched in NH_4F (40%). This procedure leads to the formation of an atomically flat H/Si-(1 $\times$1) surface.[15] Heating the samples above 700 °C results in the apparition of a sharp 2×1 RHEED pattern for Si(001) (Ref. 14) and a sharp streaky 7×7 pattern with Kikuchi lines for Si(111) [Fig. 1(a)]. Optimal growth conditions leading to the formation of high quality two-dimensional (2D) smooth Al_2O_3 films have been presented elsewhere.[13] High quality γ-Al_2O_3 layers with no silicate or SiO_2 at the Al_2O_3–Si interface are obtained for growth temperatures higher than 850 °C and oxygen pressures lower than 10^{-8} Torr to limit the thermal silicon etching through Si–O formation. Al_2O_3 grows in its γ phase on Si(001) and Si(111), which has a cubic symmetry and a spinel structure with deficiencies in aluminium and oxygen positions. The lattice parameter is equal to 0.791 nm.[16] Two different samples were grown: sample A consists of a 40 nm thick Al_2O_3 layer grown on Si(111) and sample B consists of a 6 nm thick Al_2O_3 layer grown on Si(001). The samples were studied by RHEED, TEM, and XRD. The Cu $K\alpha_1$ radiation of a Rigaku rotating anode was used as a probe for the XRD experiments.

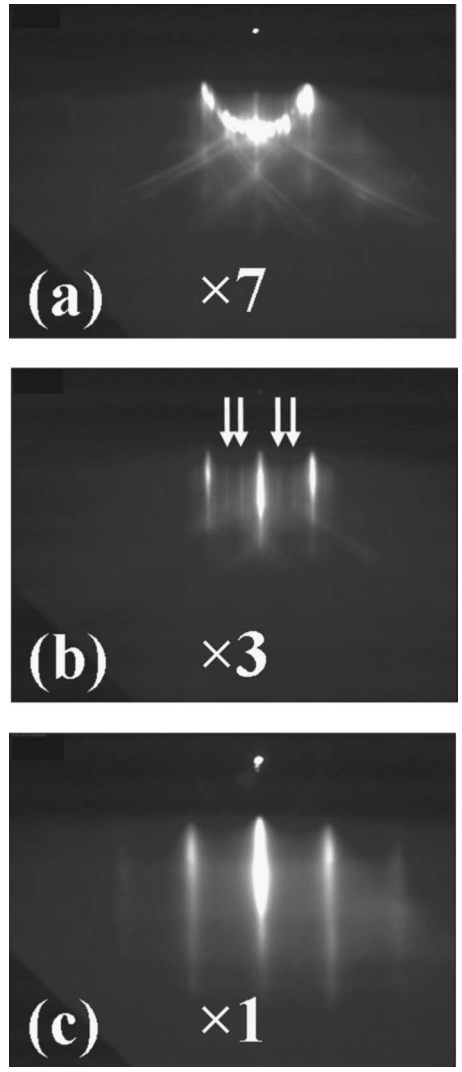

FIG. 1. RHEED patterns along the [11-2] azimuth for the Si(111)-(7×7) reconstructed surface (a), after growth of the first γ-Al_2O_3 plane leading to three times reconstruction (indicated by arrows) (b), and after growth of 40-nm-thick γ-Al_2O_3 film (c).

III. RESULTS

A. Epitaxial growth of γ-Al_2O_3 on Si(111)

The crystalline quality of sample A was *in situ* controlled using RHEED analyses. Figure 1 shows the RHEED patterns along the [11-2] azimuth for the clean Si(111) substrate [Fig. 1(a)], after growth of the first γ-Al_2O_3 monolayer [Fig. 1(b)], and after growth of 40 nm of Al_2O_3 [Fig. 1(c)]. The RHEED diagrams indicate that the 7×7 reconstructed Si(111) surface changes gradually to a reconstructed surface during the initial deposition stage of γ-Al_2O_3. Additional RHEED lines appear in 1/3 positions between the main [0,1] spots in the zero-order Laue zone corresponding to three times periodicity at the surface along the [11-2] azimuth (indicated by arrows on the RHEED diagram). During the subsequent deposition, a bright 1×1 streak pattern appears. All RHEED patterns present streak diffraction lines, showing that the growth of the alumina layer is crystalline and that the growth front remains bidimensional during the entire process. The RHEED diffraction patterns of the γ-Al_2O_3 layer present a sixfold (hexagonal) surface symmetry. This tends to indicate that (111)-oriented γ-Al_2O_3 grows on the (111)-oriented Si substrate.

Sample A was studied by x-ray diffraction. An x-ray reflectivity pattern of the sample is shown in Fig. 2(a). The strong and numerous intensity oscillations of the reflectivity spectrum are an indication of the excellent uniformity and smoothness of the film. The thickness of the Al_2O_3 film was estimated to 40 nm by fitting the oscillations. The θ-2θ XRD scan recorded in specular mode is shown in Fig. 2(b). The peaks centered at $2\theta=28.51°$, 59.01°, and 94.95° correspond to (111), (222), and (333) reflections of the Si(111) substrate, respectively. The peaks centered at $2\theta=39.43°$ and 84.85° correspond to the diffraction of the (222) and (444) planes of the γ-Al_2O_3 layer, respectively. The average out-of-plane lattice parameter of the γ-Al_2O_3 layer is $(a_\perp)Al_2O_3 = 0.791\pm0.001$ nm, as extracted from the XRD experiment. This first analyis confirms that the oxide film is a single crystal and that γ-Al_2O_3 is (111) oriented on the Si(111) substrate [γ-Al_2O_3(111)$\parallel$Si(111)]. We performed GIXRD with a 0.34° incident angle to enhance the contribution from

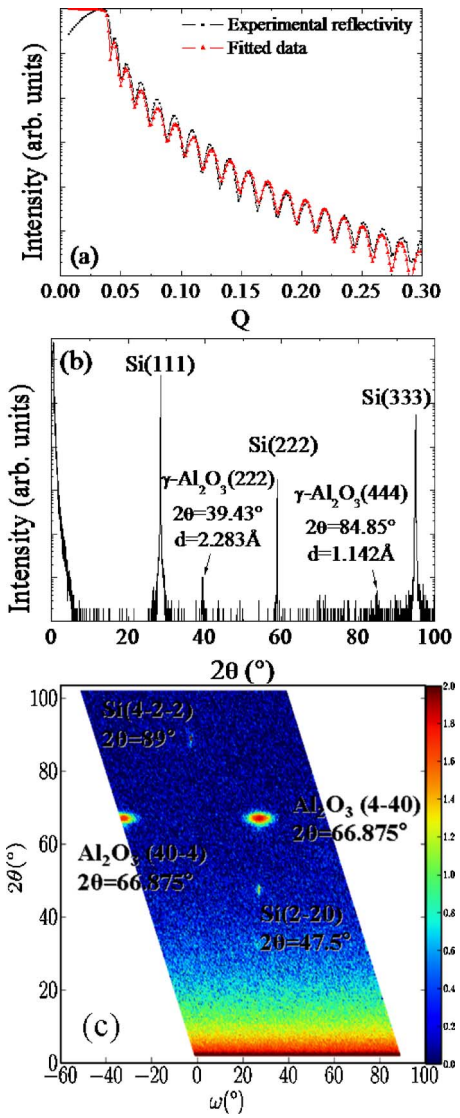

FIG. 2. (Color online) (a) Small angle reflectivity measurement determining the film thickness to be 39 nm. (b) Single crystal x-ray scan along the surface normal from a 39-nm-thick γ-Al_2O_3(111)/Si(111) heterostructure. (c) Reciprocal space cartography at grazing angles along the (111) axis perpendicular to the diffraction plane.

the epilayer. In this reciprocal map [see Fig. 2(c)] the Si(111) substrate gives sharp (2-20) and (4-2-2) peaks. The other two peaks at $2\theta=66.875°$ correspond to the Al_2O_3 phase, and are equivalent reflections (4-40) and (40-4), related to each other by a 60° rotation (omega scan) along the (111) axis perpendicular to the diffraction plane. As can be seen from the map, the (4-40) is aligned with the Si (2-20), clearly indicating the lattice match between the two lattices. The in-plane lattice parameter deduced from the 2θ position is $(a_{\parallel})Al_2O_3 = 0.791 \pm 0.003$ nm. This corresponds to a completely relaxed γ-Al_2O_3 layer (bulk parameter=0.791 nm). The in-plane epitaxial relationship between γ-Al_2O_3 and Si(111) can be deduced from the experimental results presented above. The GIXRD experiment demonstrates that the γ-Al_2O_3 (1-10) planes are aligned with the Si(1-10) planes. Moreover, the angle of 60° between two subsequent (440) Bragg reflections of γ-Al_2O_3, on the reciprocal mapping, attests of a single domain growth of alumina on (111)-oriented silicon which was already shown by RHEED.

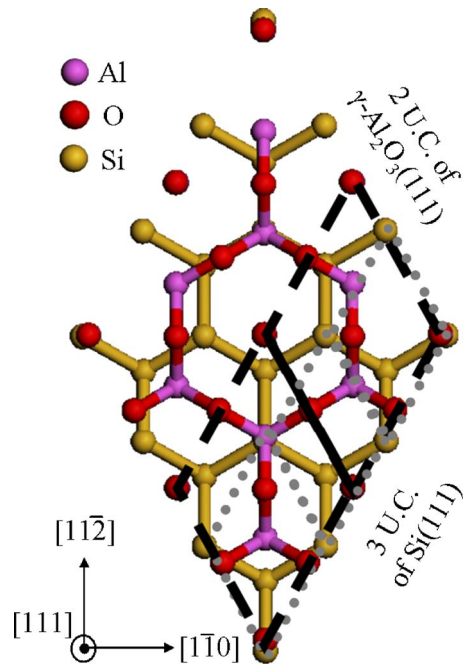

FIG. 3. (Color online) Representation of the indirect epitaxial relationship between γ-Al_2O_3(111) and Si(111).

The relative orientation of both lattices is sketched in Fig. 3, as deduced from the XRD experiments presented above. An indirect epitaxial relationship between Al_2O_3 and Si is set on by aligning two γ-Al_2O_3 unit cells (UCs) to three Si UCs. This leads to an effective lattice mismatch of −2.9%, much smaller than the cube-on-cube lattice mismatch that exceeds +45%.

Further structural informations can be extracted from the XRD experiments presented above. The (4-40) γ-Al_2O_3 Bragg reflection on the reciprocal space map consists in a diffuse reflection spot, related to the mosaicity of the γ-Al_2O_3 layer [Fig. 4(a)]. We attribute this mosaic aspect to the presence of defects generated by the plastic relaxation of the γ-Al_2O_3 on the Si substrate. To study the structural quality of the oxide layer, TEM analyses of the sample have been performed. A cross-section high resolution TEM image of the sample is shown in Fig. 4(b). This image attests of the good crystalline quality of the Al_2O_3 layer: (111) atomic planes can be distinguished in the cliché. They are parallel to the (111) atomic planes of the Si substrate, in agreement with the x-ray data of Fig. 2(b). The Si–Al_2O_3 interface is sharp at the atomic scale and continuous without pinholes. The in-plane epitaxial relationship presented above (two γ-Al_2O_3 UCs for three Si UCs) appears clearly in the inset of Fig. 4(b). There is no presence of silicates or SiO_2 despite high temperatures and high oxygen pressure used during the epitaxy process, as already demonstrated by X-ray Photoelectron Spectroscopy (XPS) analyses (not presented here, see Ref. 13). The film presents a uniform thickness of 39.5 ± 1 nm and a nearly flat surface. As already shown by the GIXRD experiments, extended defects have been detected in the 40-nm-thick alumina layer. We can observe twins inside the layer [Fig. 4(b)]. The presence of these twins was confirmed by observation of additional spots in the diffraction pattern. Actually, the twins were formed in a mirror

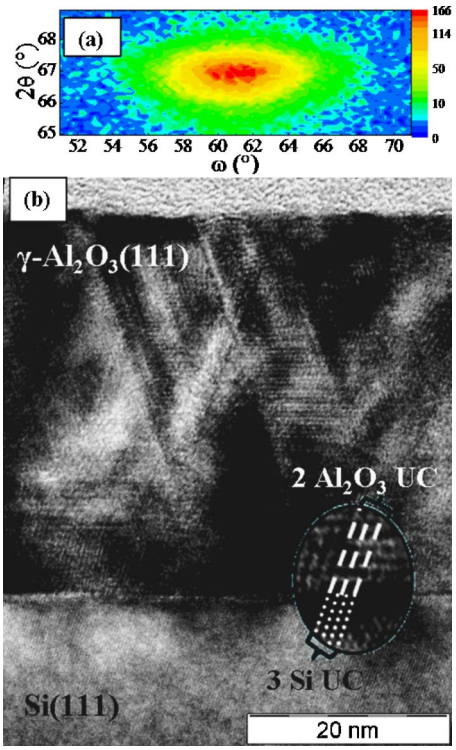

FIG. 4. (Color online) (a) Zoom of the reciprocal space map around the (4-40) Bragg reflection and (b) High resolution TEM cross-sectional image of the 39 nm-thick Al_2O_3 layer.

relation to the {111} planes parallel to the surface and to the inclined {111} planes. These defects could be at the origin of the mosaicity of the layer detected by XRD. From the diffraction patterns, we measured the interatomic distances and we concluded that the γ-Al_2O_3 was totally relaxed. The alumina lattice parameter extracted from TEM experiments is $a=0.790\pm0.005$ nm.

B. Comparison with the epitaxial growth of γ-Al_2O_3 on Si(001)

In a previous work,[14] we have demonstrated a reorientation of the γ-Al_2O_3 matrix when grown on Si(001): the first two γ-Al_2O_3 monolayers are coherently strained on the Si(001) substrate, and the γ-Al_2O_3 lattice is (001) oriented. Above a critical thickness of 1.6 nm (two monolayers), relaxation of the γ-Al_2O_3 occurs together with a spontaneous lattice reorientation: γ-Al_2O_3 becomes (111) oriented on the Si(001) substrate. The RHEED diagrams observed along the [100] and [100]+30° azimuths after the growth of the γ-Al_2O_3 layer of sample B (thickness of 6 nm) are shown in Figs 5(a) and 5(b). After the (001)-to-(111) transition, the surface presents a 12-fold symmetry with streak 1×1 reciprocal lattice rods every 30°. The brightness of the diffraction lines is an indication of the good crystallinity of the Al_2O_3 layer.

The main diffraction lines of the cliché (labeled (*i*) on the figure) correspond to the diffraction of the {11-2} planes of the Al_2O_3 layer. Additional diffraction lines, labeled (*ii*) in the figure, can be observed on the RHEED pattern. The analysis of the relative distances between these lines and the specular reflection indicate that the diffraction lines, labeled

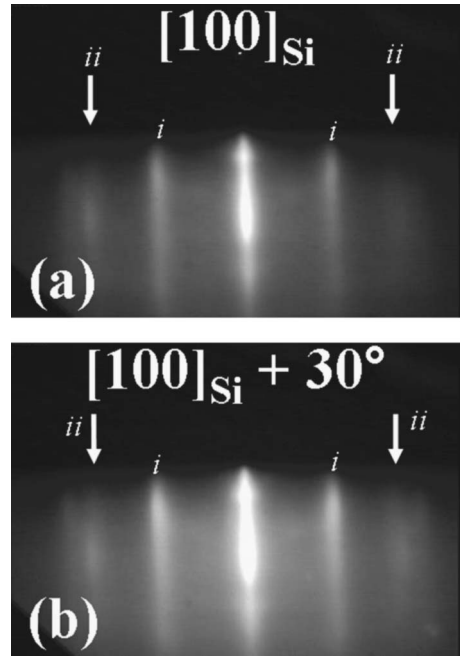

FIG. 5. RHEED patterns recorded along the $[100]_{Si}$ and $[100]_{Si}+30°$ after the growth of 6 nm of γ-Al_2O_3 [12-fold surface symmetry: (a) and (b)].

(*ii*), correspond to the diffraction of the {1-10} planes of the Al_2O_3 lattice. Thus, both the diffractions of the {-211} and {1-10} planes of Al_2O_3 can be detected along the [100] azimuth of the Si substrate. This indicates a bidomain growth of the (111)-oriented alumina layer on the Si(001) substrate for thicknesses larger than two monolayers. Two variants of the γ-Al_2O_3 lattice are present, and their orientations with respect to the Si substrate are defined by [11-2] γ-Al_2O_3(111)∥[100] Si(001) and [1-10] γ-Al_2O_3(111)∥[100] Si(001), respectively, as sketched in Fig. 6.

A TEM plane view of sample B is presented in Fig. 7. This image gives evidence of the presence of the two variants of the (111)Al_2O_3 lattice, labeled Δ1 and Δ2 in the image. The diffraction pattern corresponding to this image (not shown here, see Ref. 13) confirms the orientation of the two variants with respect to the Si substrate deduced from the RHEED patterns and sketched in Fig. 6. The average lateral extension of the domains exceeds 100 nm. Each of the variants covers approximately half of the substrate surface, indicating an equivalent probability of formation. Moreover,

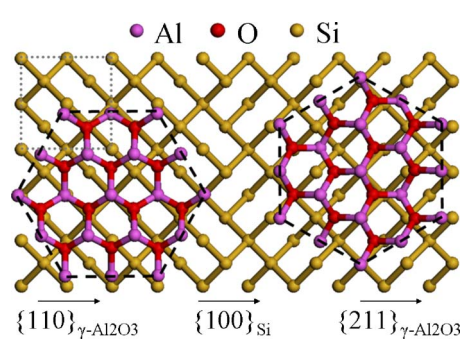

FIG. 6. (Color online) Epitaxial relationship between the Si(001) substrate and the two variants of γ-Al_2O_3(111).

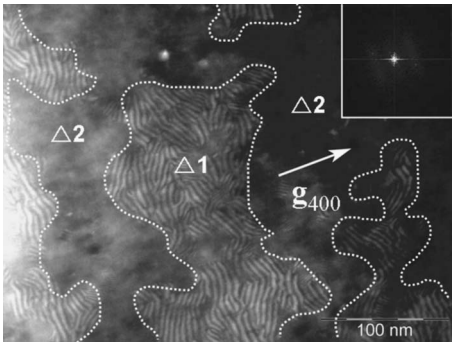

FIG. 7. TEM dark field plan view, g=400. On the right corner, the inset Fourier transform of the image shows the period of the moiré fringes. The domains corresponding to the two (111) γ-Al_2O_3 variants are labeled $\Delta 1$ and $\Delta 2$, respectively.

their geometry tends to indicate that their formation is not driven by the anisotropy of the initial dimerized silicon surface.

The plane view of Fig. 7 is taken in dark field conditions with $g_{Si}=400$. One of the 440 diffraction spots of the variant $\Delta 1$ is very close to the 400 diffraction spot of the Si. It makes the variant $\Delta 1$ matches also the Bragg conditions. It results to the formation of moiré fringes (alternate of dark and bright lines) due to the interference between the electron beams diffracted by the Si substrate and by the γ-Al_2O_3 layer. Their presence indicates that the in-plane lattice parameter of the γ-alumina layer is relaxed on Si(001). Even though the global orientation of the moiré fringes is roughly homogeneous inside the variant, the dark and bright lines present local discontinuities. Their presence reveals a slight in-plane mosaicity of the Al_2O_3 layer due to the presence of extended defects (dislocations, twins) in the layer. The in-plane lattice parameter of the γ-Al_2O_3 can be extracted from the period of the moiré fringes Δ_m. In fact, simple crystallographical considerations lead to

$$d_{440}^{\gamma\text{-}Al_2O_3} = \frac{\Delta_m}{\Delta_m/d_{400}^{Si} - 1},$$

where $d_{440}^{\gamma\text{-}Al_2O_3}=a_{par}^{\gamma\text{-}Al_2O_3}/\sqrt{32}$ and $d_{400}^{Si}=a_{par}^{Si}/4$ ($a_{par}^{\gamma\text{-}Al_2O_3}$ and a_{par}^{Si} are the in-plane lattice parameters of γ-Al_2O_3 and Si, respectively). The period of the moiré fringes Δ_m was precisely determined by measuring the intensity profile of the Fourier transform of the image (inset of Fig. 7) along the axis of modulation. We obtained a value of $\Delta_m = 4.918 \pm 0.2$ nm, which leads to $d_{440}^{\gamma\text{-}Al_2O_3}=1.3963 \pm 0.02$ Å and as a consequence $a_{par}^{\gamma\text{-}Al_2O_3}=7.90 \pm 0.11$ Å. This value is in agreement with the value determined from the diffraction patterns and very close to the bulk lattice parameter of γ-Al_2O_3 ($a=0.791$ nm). This confirms a complete in-plane relaxation of the epitaxial oxide. The resulting average crystallographic misorientation ε inside a single variant could be deduced from Fig. 7 as follows:

$$\varepsilon = \frac{d_{440}^{\gamma\text{-}Al_2O_3} - d_{400}^{Si}}{d_{400}^{Si}}\alpha,$$

where α is the apparent misorientation measured between the moiré fringes (about 30°). It leads to a crystallographic misorientation of 0.85°.

IV. DISCUSSION

The study related here evidences the strong influence of the substrate orientation on the growth of γ-Al_2O_3 (spinel structure) on Si. Single domain (111)-oriented alumina grows on Si(111), with indirect epitaxial relationship (two UCs of alumina for three UCs of Si). On Si(001), the growth mechanism is more complex: the first two monolayers are strained and (001)-oriented on the substrate, and further growth leads to a bidomain growth of (111)-oriented Al_2O_3. This strong influence of the substrate orientation is typical for the epitaxial growth of materials, which crystal structure differs from the one of the substrate, and has already been observed in some oxide/Si systems. For $SrTiO_3$ (STO) (perovskite structure), a single domain growth is observed on Si(001) substrate with an in-plane rotation of 45° of the perovskite lattice with respect to the Si substrate.[17] However, STO is (110) oriented on Si(111) substrates, leading to the formation of three different domains.[18] Similarly, single domain (111)-oriented Gd_2O_3 (bixbyite structure) grows on Si(111), with a cube-on-cube epitaxial relationship (one UC of Gd_2O_3 for two UCs of Si).[19] On Si(001), Gd_2O_3 is (110) oriented leading to a bidomain growth.[20] The origin of the onset of such orientations and indirect epitaxial relationships is not clearly understood. The connetion between the oxide lattice and the Si substrate takes place via the oxygen sublattice of the oxide.[21] The configuration of the latter is a key parameter for the orientation of the oxide with respect to Si that will mainly result from a minimization of the mismatch and interface energies. The surface energies of the oxide and substrate are also expected to play a predominant role.

The behavior of γ-Al_2O_3 grown on Si brings some elements for the understanding of the growth of oxides on Si. In particular, the observation of a lattice reorientation on Si(001) is original. One possible explanation for this reorientation could be that both orientations of alumina coexist at the beginning of the growth, and that the (111) orientation becomes predominant after two monolayers due to a strong difference in the growth rates of (001)- and (111)-oriented Al_2O_3. However, our experiments indicate a relative brutal transition in the growth orientation, incompatible with such a mechanism. We therefore attribute the observation of this transition in the growth orientation to an energetic balance between the cost in energy related to the reorientation of the lattice (formation of dislocations and/or breaking of atomic bonds) and the gain in energy related to the development of a stable (111) surface. The driving force for this transition is attributed to the elastic energy accumulated in the first two monolayers of γ-Al_2O_3, which orientation is imposed by the Si(001) substrate. However, further investigations are required to fully understand the growth mechanism.

V. CONCLUSION

In this work, the growth of γ-Al_2O_3 has been investigated on different silicon substrate orientations. On Si(111), we obtain high quality growth of γ-Al_2O_3(111), with good crystalline properties and a two-for-three unit cell favorable epitaxial relationship. The growth is then a single domain. On Si(001), the first two monolayers of γ-Al_2O_3 grow with a

cube-on-cube-like epitaxial relationship and are coherently strained on Si. Increasing the alumina thickness above 1.6 nm leads to a transition from (001) to (111) planes in the growth direction. This is associated with the apparition of a bidomain in the alumina layer. This transition is attributed to the gain in energy related to the development of the (111) alumina surface.

ACKNOWLEDGMENTS

The authors would like to thank Ph. Regreny and M. Gendry for helpful discussions as well as C. Botella and J. B. Goure for technical assistance. This work was supported by the NANO2008 Project and by the European Commission's Information Society Technologies Programme, under PULLNANO Project Contract No. IST-026828.

[1]G. D. Wilk, R. M. Wallace, and J. M. Anthony, J. Appl. Phys. **89**, 5243 (2001).
[2]H. J. Osten, J. P. Liu, E. Bugiel, H. J. Müssig, and P. Zaumseil, Mater. Sci. Eng., B **87**, 297 (2001).
[3]R. Droopad *et al.*, J. Cryst. Growth **251**, 638 (2003).
[4]R. A. McKee, F. J. Walker, J. R. Conner, E. D. Specht, and D. E. Zelmon, Appl. Phys. Lett. **59**, 782 (1991).
[5]G. Delhaye *et al.*, J. Appl. Phys. **100**, 124109 (2006).
[6]T. Okada, M. Shahjahan, K. Sawada, and M. Ishida, Jpn. J. Appl. Phys., Part 1 **44**, 2320 (2005).
[7]C. Merckling *et al.*, Microelectron. Reliab. **47**, 540 (2007).
[8]K. Sawada, M. Ishida, T. Nakamura, and N. Ohtake, Appl. Phys. Lett. **52**, 1672 (1988).
[9]S. Y. Wu, M. Hong, A. R. Kortan, J. Kwo, J. P. Mannaerts, W. C. Lee, and Y. L. Huang, Appl. Phys. Lett. **87**, 091908 (2005).
[10]T. Okada, M. Ito, K. Sawada, and M. Ishida, J. Cryst. Growth **290**, 91 (2006).
[11]M. Ishida, I. Katakabe, T. Nakamura, and N. Ohtake, Appl. Phys. Lett. **52**, 1326 (1988).
[12]H. Wado, T. Shimizu, and M. Ischida, Appl. Phys. Lett. **67**, 2200 (1995).
[13]C. Merckling, M. El-Kazzi, V. Favre-Nicolin, M. Gendry, Y. Robach, G. Grenet, and G. Hollinger, Thin Solid Films **515**, 6479 (2007).
[14]C. Merckling, M. El-Kazzi, G. Delhaye, L. Largeau, G. Patriarche, M. Gendry, G. Saint-Girons, and G. Hollinger, Appl. Phys. Lett. **89**, 232907 (2006).
[15]V. Le Thanh, M. Eddrief, C. A. Sebenne, P. Dumas, A. Taleb-Ibrahimi, R. Gunther, Y. J. Chabal, and J. Derrien, Appl. Phys. Lett. **64**, 3308 (1994).
[16]H. P. Pinto, R. M. Nieminen, and S. D. Elliott, Phys. Rev. B **70**, 125402 (2004).
[17]R. A. McKee, F. J. Walker, and M. F. Chisholm, Phys. Rev. Lett. **81**, 3014 (1998).
[18]Y. Machida, H. Asaoka, H. Yamamoto, and S. Shamoto, Surf. Sci. **600**, 724 (2006).
[19]A. Fissel, Z. Elassar, O. Kirfel, E. Bugiel, M. Czernohorsky, and H. J. Osten, J. Appl. Phys. **99**, 074105 (2006).
[20]A. Laha, E. Bugiel, H. J. Osten, and A. Fissel, Appl. Phys. Lett. **88**, 172107 (2006).
[21]A. Fissel, H. J. Osten, and E. Bugiel, J. Vac. Sci. Technol. B **21**, 1765 (2003).